Title
A VTVH MCD and EPR Spectroscopic Study of the Maturation of the “Second” Nitrogenase P-Cluster

Journal
Inorganic Chemistry, 57(8)

ISSN
0020-1669

Authors
Rupnik, Kresimir
Lee, Chi Chung
Hu, Yilin
et al.

Publication Date
2018-04-16

DOI
10.1021/acs.inorgchem.8b00428

Peer reviewed

HHS Public Access

Author manuscript

Inorg Chem. Author manuscript; available in PMC 2019 April 16.

Published in final edited form as:

Inorg Chem. 2018 April 16; 57(8): 4719–4725. doi:10.1021/acs.inorgchem.8b00428.

A VTVH MCD and EPR Spectroscopic Study of the Maturation of the "Second" Nitrogenase P-Cluster

Kresimir Rupnik[†], **Chi Chung Lee**[§], **Yilin Hu**[§,*], **Markus W. Ribbe**[§,*], and **Brian J. Hales**[†,*]

[§]Department of Molecular Biology and Biochemistry, University of California, Irvine, CA 92697

[†]Department of Chemistry, Louisiana State University, Baton Rouge, LA 70808

Abstract

The P-cluster of the nitrogenase MoFe protein is a [Fe_8S_7] cluster that mediates efficient transfer of electrons to the active site for substrate reduction. Arguably the most complex homometallic FeS cluster found in nature, the biosynthetic mechanism of the P-cluster is of considerable theoretical and synthetic interest to chemists and biochemists alike. Previous studies have revealed a biphasic assembly mechanism of the two P-clusters in the MoFe protein upon incubation with Fe protein and ATP, in which the first P-cluster is formed through fast fusion of a pair of [Fe_4S_4]$^+$ clusters within 5 min and the second P-cluster is formed through slow fusion of the second pair of [Fe_4S_4]$^+$ clusters in a period of 2 h. Here we report a VTVH MCD and EPR spectroscopic study of the biosynthesis of the slow-forming, second P-cluster within the MoFe protein. Our results show that the first major step in the formation of the second P-cluster is the conversion of one of the precursor [Fe_4S_4]$^+$ clusters into an integer spin cluster [$Fe_4S_{3\text{-}4}$]$^{\alpha}$, a process aided by the assembly protein NifZ; whereas the second major biosynthetic step appears to be the formation of a diamagnetic cluster with a possible structure of [$Fe_8S_{7\text{-}8}$]$^{\beta}$, which is eventually converted into the P-cluster.

Graphical abstract

*Corresponding Authors: bhales@lsu.edu; mribbe@uci.edu ; yilinh@uci.edu.

The authors declare no competing financial interests.

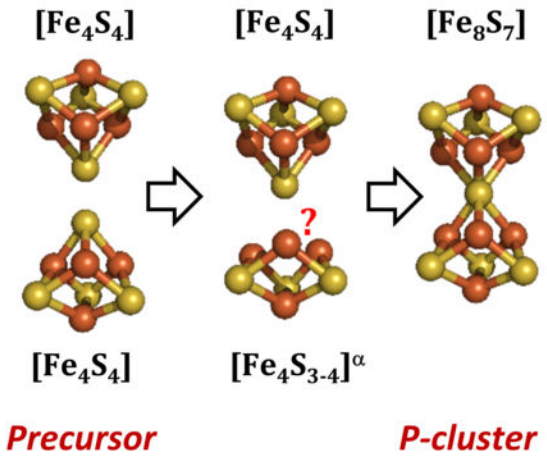

An Electron Paramagnetic Resonance/Magnetic Circular Dichroism spectroscopic study of the maturation of the two $[Fe_4S_4]^+$ precursor clusters on the nitrogenase MoFe protein (NifDK) into the second P-cluster (Fe_8S_7) reveals that the first step of the reaction is the conversion of one of the $[Fe_4S_4]^+$ clusters into an integer spin cluster, possibly the all-ferrous cluster $[Fe_4S_4]^0$.

Nitrogen fixation, the biological conversion of dinitrogen to ammonia, is catalyzed by the enzyme nitrogenase[1]. The best characterized form of this enzyme, Mo-nitrognease, consists of two separable proteins, the Fe protein (encoded by *nifH*) and the MoFe protein (encoded by *nifDK*), both of which are required for the enzymatic activity of nitrogenase. The Fe protein is a γ_2 homodimer containing one MgATP binding site within each subunit and a subunit-bridging $[Fe_4S_4]$ cluster[2]. The MoFe protein is an $\alpha_2\beta_2$ tetramer housing two pairs of metal clusters: the P-cluster and the FeMo-cofactor (or FeMoco). The P-cluster is a $[Fe_8S_7]$ unit bridging each αβ dimer (Figure 1A, B), whereas the FeMoco is a [*MoFe*$_7$*S*$_9$*C-homocitrate*] cluster located within each α subunit[3–5]. During catalysis, electrons are transferred from the P-cluster to the FeMoco of the MoFe protein[6], where substrate reduction takes place followed by transfer from the $[Fe_4S_4]$ cluster of the Fe protein to the P-cluster concomitant with ATP hydrolysis.

The assembly of P-cluster, the “capacitor” mediating the electron transfer to the FeMoco during catalysis, has attracted considerable attention[9–10]. The precursor of the P-cluster was identified through the characterization of a FeMoco-deficient MoFe protein (designated Δ*nifH* MoFe protein)[7–11] generated *in vivo* upon deletion of *nifH*, the gene encoding the Fe protein that is essential for FeMoco maturation. The Δ*nifH* MoFe protein contains two pairs of neighboring $[Fe_4S_4]$-like clusters (Figure 1C) at the equivalent positions of the two P-clusters[7–11]. In Nature, these clusters can exist in four different paramagnetic states, $[Fe_4S_4]^0$ ($S = 4$), $[Fe_4S_4]^+$ ($S = ½, 3/2, 5/2$), $[Fe_4S_4]^{2+}$ ($S \geq 1$ or 0) and $[Fe_4S_4]^{3+}$ ($S = ½$)[12–14]. Most surprisingly, chemical oxidation of the all-ferrous clusters can convert the precursors into P-clusters in a non-enzymatic reaction[14].

The biosynthesis of the P-cluster can be studied through incubation of Δ*nifH* MoFe protein with Fe protein, ATP, and reductant[11, 15]. The time-dependent profile of P-cluster biosynthesis in Δ*nifH* MoFe protein reveals that this process occurs in two phases: an initial fast phase (0-5 min), during which one P-cluster is synthesized; and a second slow phase (*ca.* 2 h), during which the second P-cluster is formed[15–16]. To date, details of the mechanism for the formation of either cluster are unknown.

The assembly of the second P-cluster can be further investigated through the characterization of another FeMoco-deficient MoFe protein (designated Δ*nifBZ* MoFe protein), which is generated *in vivo* upon deletion of *nifB* and *nifZ*, the genes encoding proteins essential for the synthesis of the FeMoco and the second P-cluster, respectively[17–18]. The Δ*nifBZ* MoFe protein contains one complete P-cluster and a [Fe_4S_4] cluster pair, like that found in the Δ*nifH* MoFe protein, at the second P-cluster site[17]. The biosynthesis of the second P-cluster can be achieved through incubation of the Δ*nifBZ* MoFe protein with NifZ, followed by incubation of this protein with Fe protein, ATP, and reductant. The time-dependent profile of the P-cluster synthesis in Δ*nifBZ* MoFe protein is essentially identical to that of the second P-cluster in Δ*nifH* MoFe protein, suggesting that both reactions follow the same mechanism[11].

In this work, we use variable-temperature, variable-field magnetic circular dichroism (VTVH MCD) and EPR spectroscopies to further explore the formation of the second P-cluster in both Δ*nifBZ* and Δ*nifH* MoFe proteins. Our results show that the formation of the second P-cluster undergoes an initial conversion of one of the precursor [Fe_4S_4]$^{+}$ clusters into an integer spin cluster [$Fe_4S_{3\text{-}4}$]$^{\alpha}$ in a process facilitated by NifZ, followed by possible formation of a diamagnetic cluster with a proposed structure [$Fe_8S_{7\text{-}8}$]$^{\beta}$ prior to conversion of this intermediate into a mature P-cluster.

Results

Biosynthesis of the second P-cluster in ΔnifBZ MoFe protein.

The MCD spectrum of the reduced Δ*nifBZ* MoFe protein has been published previously[17] and shown to exhibit the classic inflections and amplitude of two [Fe_4S_4]$^{+}$ clusters. The magnetization curves of Δ*nifBZ* MoFe protein can be simulated by adding ½ of the spectrum of reduced Δ*nifH* MoFe protein (representing two [Fe_4S_4]$^{+}$ clusters) and ½ of the spectrum of reduced Δ*nifB* MoFe protein (representing one diamagnetic P-cluster, designated P^N), consistent with the characterization of a MoFe protein containing two [Fe_4S_4]$^{+}$ clusters and one complete P-cluster.

The MCD spectrum of oxidized Δ*nifBZ* MoFe protein (Figure 2), on the other hand, has not been reported so far. Like the spectrum of the reduced protein, the spectrum of the oxidized protein can be simulated by adding ½ of the spectrum of the oxidized Δ*nifH* MoFe protein (representing two paramagnetic [Fe_4S_4]$^{2+}$ clusters) and ½ of the spectrum of the oxidized Δ*nifB* MoFe protein (representing one paramagnetic oxidized P-cluster, designated P^{2+}). Therefore, the simulations of both reduced and oxidized proteins clearly verify that Δ*nifBZ* MoFe protein contains one complete P-cluster and two neighboring [Fe_4S_4] clusters that are electronically and structurally identical to those in the precursor Δ*nifH* MoFe protein.

Figure 3 shows the MCD spectrum of the reduced Δ*nifBZ* MoFe protein following incubation with NifZ (designated Δ*nifBZ* MoFe protein^{+NifZ}). The electronic structure of the cluster species in Δ*nifBZ* MoFe protein^{+NifZ} clearly arises from a $[Fe_4S_4]^+$ cluster[19], with its inflections in the MCD spectrum being essentially identical to those in both Δ*nifBZ* and Δ*nifH* MoFe proteins. However, unlike Δ*nifBZ* and Δ*nifH* MoFe proteins that exhibit distinct $S = ½$ EPR signals, the Δ*nifBZ* MoFe protein^{+NifZ} is practically EPR silent (Figure 4). These remaining signals consist of a small radical-like g 2 signal and a rolling background distinctly different from the original Δ*nifBZ* signal. The source of these signals is unknown.

A comparison between the magnetization curves of Δ*nifBZ* MoFe protein with those of Δ*nifBZ* MoFe protein^{+NifZ} (Figure 5) reveals that, while the curves of Δ*nifBZ* MoFe protein exhibit the general shape associated with the $S = ½$, $[Fe_4S_4]^+$ clusters with a small linear diamagnetic contribution due to the presence of the P-cluster ($S = 0$)[17], the curves of Δ*nifBZ* MoFe protein^{+NifZ} exhibit complex fluctuations with both temperature and magnetic field. These fluctuations suggest the presence of a second paramagnetic species, different from the normal $S = ½$ $[Fe_4S_4]^+$ cluster, in Δ*nifBZ* MoFe protein^{+NifZ}.

The MCD spectrum of the oxidized Δ*nifBZ* MoFe protein^{+NifZ} (Figure 6) shows both similarities and differences when compared with that of the oxidized Δ*nifBZ* MoFe protein. On the one hand, both proteins are similar in that they exhibit a strong spectral inflection at 800 nm that is associated with a single oxidized P-cluster (P^{2+}). On the other hand, the inflections associated with the two paramagnetic $[Fe_4S_4]^{2+}$ clusters in Δ*nifBZ* MoFe protein are absent from the spectrum of the oxidized Δ*nifBZ* MoFe protein^{+NifZ}.

Biosynthesis of the second P-cluster in ΔnifH MoFe protein.

The biphasic formation of the two P-clusters in Δ*nifH* MoFe protein was monitored by EPR and MCD spectroscopic techniques. Consistent with the formation of P-clusters, the MCD spectrum of the oxidized Δ*nifH* MoFe protein (Figure 7) exhibits a broad transition at 800 nm (mainly due to P^{2+}) that increases in intensity with the incubation time of Δ*nifH* MoFe protein with Fe protein, ATP and reductant. Parallel mode EPR spectroscopy of Δ*nifH* MoFe protein[16] shows a similar increase in intensity of the signal at $g = 11.9$ with incubation time, which is characteristic of the P^{2+} state of the P-cluster.

A similar study of reduced Δ*nifH* MoFe protein reveals even more interesting details. Magnetization curves recorded at 0 min (Figure 8) exhibit shapes characteristic of predominately an $S = ½$ system, consistent with the EPR spectrum and previous MCD spectroscopic studies[12]. At 5 and 20 min of incubation, however, the magnetization curves exhibit strong deviation from a simple $S = ½$ system, similar to the curves obtained for Δ*nifBZ* MoFe protein^{+NifZ} (Figure 5).

Figure 9 shows the MCD spectrum of Δ*nifH* MoFe protein after 5 min of incubation, when approximately one pair of $[Fe_4S_4]$ clusters is converted into a P-cluster and the second pair of $[Fe_4S_4]$ clusters remains in the precursor state. Interestingly, the MCD spectrum exhibits inflections characteristic of $[Fe_4S_4]^+$ clusters with a spectral intensity suggesting *ca.* 1.4 clusters per protein; whereas the EPR spectrum associated with the $[Fe_4S_4]^+$ clusters is

much smaller, corresponding to *ca.* 0.3 clusters per protein. While the MCD spectral amplitudes correlate with the concentration of $[Fe_4S_4]^+$ clusters, EPR spectral intensities can be diminished (e.g., broadened) by the presence of strong dipolar and exchange interactions. Similar interactions may also be present in Δ*nifBZ* MoFe protein^{+NifZ} and may account for the lack of a significant EPR spectrum in that protein. After 20 min of incubation, the MCD spectral intensity of the $[Fe_4S_4]^+$ clusters in Δ*nifH* MoFe protein continues to decrease as more P-clusters are formed. Surprisingly, the MCD signal intensity increases again at 60 min of incubation with a further increase at 120 min.

Discussion

Effect of incubating ΔnifBZ MoFe protein with NifZ.

NifZ is a small (19 kDa), non-redox-active protein that has been shown to be essential for the biosynthesis of the second, slow-forming P-cluster. However, while NifZ must interact with Δ*nifBZ* MoFe protein to enable the formation of the second P-cluster, it does not have to be present during the subsequent coupling of two $[Fe_4S_4]$ clusters into a mature P-cluster.

The MCD spectrum of Δ*nifBZ* MoFe protein^{+NifZ} exhibits inflections similar to those of both Δ*nifH* and Δ*nifBZ* MoFe proteins (Figure 3). What is different among these spectra is their intensity. The spectral intensity at 520 nm of a typical $[Fe_4S_4]^+$ cluster[20–21] is 60–90 $\Delta\varepsilon\ M^{1-}\ cm^{1-}$. Using that parameter, the intensity of the Δ*nifH* MoFe protein spectrum correlates to four $[Fe_4S_4]^+$ clusters, consistent with the previous biochemical and spectroscopic analysis of this protein. Likewise, consistent with the presence of only two $[Fe_4S_4]^+$ clusters in Δ*nifBZ* MoFe protein, the spectral intensity of this protein is approximately half (~46%) of that of Δ*nifH* MoFe protein. Unexpectedly, the spectral intensity of Δ*nifBZ* MoFe protein^{+NifZ} is only one fourth (~27%) of that of Δ*nifH* MoFe protein, suggesting the presence of only one $[Fe_4S_4]^+$ cluster rather than the expected two in this protein.

What happened to the second $[Fe_4S_4]^+$ cluster? The complexity of the magnetization curves of Δ*nifBZ* MoFe protein^{+NifZ}, when compared to those of the Δ*nifBZ* MoFe protein, shows that the cluster species in Δ*nifBZ* MoFe protein^{+NifZ} is not a pure $S = ½$ system and suggests the presence of a second high-spin paramagnetic cluster. Additionally, Δ*nifBZ* MoFe protein $^{+NifZ}$ is essentially EPR-silent, further suggesting that the second cluster became high-spin paramagnetic, which would likely induce spectral broadening through dipolar and/or exchange interactions.

The logical conclusion is that the second cluster is an integer spin (non-Kramer) state. But, if the second cluster is paramagnetic, why does it contribute little, if any, intensity to the MCD spectrum at 1.6 K? One answer to that question is that the second cluster could be an integer spin state with a near axial ($E \approx 0$) symmetry and positive zero-field splitting, $D > 0$. In that situation, the ground state would be non-degenerate ($m_s = 0$) and would, therefore, contribute almost no MCD spectral intensity[19] at 1.6 K. As the temperature rises, degenerate excited states (e.g., $m_s = \pm 1$) would become populated and contribute to both the MCD spectrum and magnetization curves. This is consistent with the data showing that the

magnetization curve of the Δ*nifBZ* MoFe protein^{+NifZ} at 1.6 K nearly mimics an $S = ½$ system but deviates dramatically at higher temperatures (Figure 5).

Another possibility is that the second cluster has become an all-ferrous, $[Fe_4S_4]^0$ cluster. The $[Fe_4S_4]^0$ cluster has been previously shown to be an intermediate in the non-enzymatic synthesis of the P-cluster[14] and, as such, may also be an intermediate in the biosynthesis of this cluster. The ground state of $[Fe_4S_4]^0$ is typically paramagnetic with $S = 4$ ($D < 0$), as verified by EPR and Mössbauer spectroscopic studies. The possibility that the second cluster is $[Fe_4S_4]^0$ can be easily tested through spectral simulation. The MCD spectrum of the dithionite-reduced Δ*nifBZ* MoFe protein corresponds to two $[Fe_4S_4]^+$ clusters, while the spectrum of the Ti(III) citrate reduced Δ*nifH* MoFe protein corresponds to four $[Fe_4S_4]^0$ clusters[14]. Adding ½ the spectrum of the dithionite-reduced Δ*nifBZ* MoFe protein and ¼ of the spectrum of Ti(III) citrate-reduced protein should closely simulate the spectrum of Δ*nifBZ* MoFe protein^{+NifZ}, assuming the protein in question contains one $[Fe_4S_4]^+$ cluster and one $[Fe_4S_4]^0$ cluster.

Figure 10 shows the simulated spectrum at 1.6 K, which yields a very good fit to the experimental spectrum of Δ*nifBZ* MoFe protein^{+NifZ}. The reason for this close fit is easy to explain. The transitions in the MCD spectrum of $[Fe_4S_4]^0$ are similar to those of $[Fe_4S_4]^+$ but with much lower intensity (all of the iron in $[Fe_4S_4]^0$ are ferrous, thus reducing the presence of the normally dominant S-to-Fe charge-transfer bands in the spectrum). Therefore, adding the two spectra yields a spectrum only slightly larger than that of a single $[Fe_4S_4]^+$ cluster. As the temperature increases, the relative spectral contribution of the high-spin $S = 4$ $[Fe_4S_4]^0$ cluster will increase compared to that of the low-spin $S = ½$ $[Fe_4S_4]^+$ cluster, resulting in magnetization curves that greatly deviate from an $S = ½$ system at higher temperatures (Figure 8).

Biosynthesis of the second P-cluster in ΔnifH MoFe protein.

The overall synthesis reaction is the conversion of two neighboring $[Fe_4S_4]^+$ clusters (collectively abbreviated as ***P****) in Δ*nifH* MoFe protein into the P-cluster (abbreviated as ***P***). Three basic mechanisms can be proposed for the synthesis of the second P-cluster: *No Intermediates*

$$\boldsymbol{P}^* \xrightarrow{k_{01}} \boldsymbol{P} \quad (1)$$

One Intermediate

$$\boldsymbol{P}^* \xrightarrow{k_{11}} A \xrightarrow{k_{12}} \boldsymbol{P} \quad (2)$$

Two Intermediates

$$\boldsymbol{P}^{*} \xrightarrow{k_{21}} \boldsymbol{A} \xrightarrow{k_{22}} \boldsymbol{B} \xrightarrow{k_{23}} \boldsymbol{P} \quad (3)$$

Best-fit simulations of the experimental data were performed (see Supporting Information) for each mechanism.

It is obvious that the experimental data do not fit the simulation (Figure 11) for Equation (1). Equations (2) and (3) provide better fits of the data, with Equation (3) showing the best fit of the three. For the sake of simplicity and discussion only, it will be assumed that the reaction mechanism has two intermediates (Equation 3). However, mechanisms with more intermediates cannot be excluded.

As discussed above, MCD spectroscopy is an excellent technique for monitoring the concentration of $[Fe_4S_4]^+$ clusters. At 5 min of synthesis the protein should contain approximately one P-cluster, which is diamagnetic and, therefore contribute only slightly to the MCD spectrum[12]. This means that the MCD spectra at 5, 20, 60 and 120 min mainly reflect paramagnetic intermediates in the synthesis of the second P-cluster. The two-intermediate kinetic scheme (Equation 3) predicts (Figure S1) that components ***P**** and ***A*** will dominate the MCD spectrum at 5 min. The magnetization curves at the 5 min synthesis mark (Figure 8) exhibit fluctuations similar to those of Δ*nifBZ* MoFe protein$^{+\mathrm{NifZ}}$ (Figure 5), suggesting that both proteins contain similar paramagnetic clusters. These fluctuations are even more pronounced at 20 min (Figure 8). This suggests that the first major step of ***P**** to ***A*** in the reaction mechanism for the biosynthesis of the second P-cluster is likely the conversion of one $[Fe_4S_4]$ cluster into an integer spin cluster, $[Fe_4S_{3-4}]^{\alpha}$.

One of the most interesting features of the data collected on reduced Δ*nifH* MoFe protein is the increase in the MCD spectral concentration during the later stages of P-cluster biosynthesis. Specifically, the initial $[Fe_4S_4]^+$-like signal intensity decreases during the first 20 min but then increases with time. Obviously, the increase of the signal intensity cannot correspond to the original $[Fe_4S_4]^+$ clusters since those clusters have been converted into P-clusters by 120 min; rather, such an increase must originate from some other FeS cluster species.

Since there are no other proteins present, it is possible that the signal originates from the newly formed second P-cluster. It has been shown that the one-equivalent oxidized P-cluster (P^+) yields MCD and EPR spectra characteristic of $[Fe_4S_4]^+$-like clusters[22]. Therefore, if the second P-cluster forms as P^+ rather than P^N, the intensity of the new $[Fe_4S_4]^+$-like signal will correlate with the concentration of the second P-cluster. This correlation is demonstrated using the theoretical kinetic equations (i.e., Equations SE7, SE12, SE13 and SE 14) to predict the variation in the intensity of the total $[Fe_4S_4]^+$-like MCD signals with time (see Supporting Information).

Figure 12 plots the MCD data (amplitude at 520 nm) along with the predicted MCD spectral intensity using the assumption that the new $[Fe_4S_4]^+$-like signal correlates with the formation of the second P-cluster (see Supporting Information).

The final question is the identity of intermediate ***B*** (Eq. 4). Because ***B*** is generated in the middle of the synthesis, at a time point when ***P****, ***A***, ***B*** and ***P*** are all present, it is much more difficult to isolate and characterize ***B***. The theoretical reaction profile (Figure S2) suggests that ***B*** reaches its maximum intensity between the 20 min and 60 min synthesis marks. However, during that time period, no new inflections are observed in the MCD spectrum of the reduced protein, which suggests that ***B*** may be diamagnetic. The MCD spectra of the oxidized system, on the other hand, exhibit new inflections (Figure 9) in the 400–600 nm region, which are different from those associated with pure P^{2+}. The perpendicular mode EPR spectrum (Figure S3) of the oxidized system also shows inflections in the g 2 region that grow in intensity with time, maximizing at 60 min yet barely detectable at 120 min. The MCD and EPR spectral inflections may correspond to $\boldsymbol{B}^{+}$ or some other intermediate generated later in the biosynthesis of the P-cluster. Unfortunately, neither the EPR nor the MCD spectrum allows identification of the structure of ***B***. However, it could be proposed that ***B*** represents a fusion of the ***A*** clusters into a structure ($[Fe_8S_{7\text{-}8}]^{\beta}$) similar to the P-cluster.

Summary

Simulations of the biosynthetic reaction profile of the second P-cluster suggest the appearance of at least two major intermediates during the formation of this P-cluster. One of the initial intermediates (***A***) appears to involve the conversion of one of the precursor $[Fe_4S_4]^{+}$ clusters into an integer spin cluster, possibly with the loss of an S atom (i.e., $[Fe_4S_3]^{\alpha}$). The mechanism for the removal of the surplus sulfide is unclear, although it can be speculated that this sulfide is removed as H_2S or a protein-bound persulfide. The identity of the new cluster is likely either an integer spin state with near axial symmetry ($E \sim 0$ and $D > 0$) or the all-ferrous, $[Fe_4S_4]^{0}$ cluster. The current MCD and EPR spectroscopic data are unable to definitively favor one or the other of these two proposed structures for the new cluster. Another major intermediate (***B***) is more difficult to characterize. The lack of either an obvious MCD or EPR spectrum suggests it as a diamagnetic multinuclear cluster, possibly representing a fusion of the two original clusters into an 8Fe precursor of the eventual P-cluster.

Questions still remain as to why the synthesis of only the second P-cluster requires NifZ and why the formation kinetics of the two P-clusters are so different. It is unlikely that the formation kinetics of the second P-cluster is significantly slower that the first P-cluster in vivo. The in vivo P-cluster maturation could be facilitated by the physiological electron donor(s), which deliver electrons more efficiently to the Fe protein and/or render the Fe protein in an appropriate redox state/conformation for the subsequent reductive coupling of the 4Fe precursors into a P-cluster. A similar discrepancy between the in vivo and in vitro activities has been observed in the case of CO_2 reduction to CO by A. vinelandii Fe proteins, where the turnover number of the in vitro assay (where dithionite is supplied as an electron source) is considerably lower than that under the in vivo conditions[23]. Moreover, chaperon proteins, such as GroEL, have been implicated in the nitrogenase maturation process[24]. Therefore, the possible participation of chaperons and other accessory proteins in this process in vivo cannot be excluded. While NifZ has been proposed to act as a clamp that prepares the site of the second P-cluster for maturation, the implication of the two

introductory questions suggests a cooperative interaction between the clusters even though they are ca. 60 Å apart and thereby provide a basic framework for further investigations into the mechanistic details of P-cluster biosynthesis in the future.

Supplementary Material

Refer to Web version on PubMed Central for supplementary material.

ACKNOWLEDGEMENTS

This work was supported by NIH-NIGMS grant GM67626 (to M.W.R. and Y.H.)

References

1. Burgess BK; Lowe DJ, Mechanism of Molybdenum Nitrogenase. Chem. Rev 1996**,** 96, 2983–3011. [PubMed: 11848849] **,**
2. Georgiadis MM; Komiya H; Chakrabarti P; Woo D; Kornuc JJ; Rees DC, Crystallographic Structure of the Nitrogenase Iron Protein from *Azotobacter vinelandii*. Science 1992**,** 257, 1653–1659. [PubMed: 1529353] **,**
3. Einsle O; Tezca FA; Andrade SLA; Schmid B; Yoshida M; Howard JB; Rees DC, Nitrogenase MoFe-Protein at 1.16 Å Resolution: A Central Ligand in the FeMo-Cofactor. Science 2002, 297, 1696–1700. [PubMed: 12215645]
4. Spatzal T; Aksoyoglu M; Zhand L; Andrade SLA; Schleicher E; Weber S; Rees DC; Einsle O, Evidence for Interstitial Carbon in Nitrogenase FeMo Cofactro. Science 2011, 334, 940. [PubMed: 22096190]
5. Lancaster KM; Roemelt M; Ettenhuber P; Hu Y; Ribbe MW; Neese F; Bergmann U; DeBeer S, X-Ray Emission Spectroscopy Evidences a Central Carbon in the Nitrogenase Iron-Molybdenum Cofactor. Science 2011, 334, 974–977. [PubMed: 22096198]
6. Danyal K; Dean DR; Hoffman BM; Seefeldt LC, Electron Transfer within Nitrogenase: Evidence for a Deficit-Spending Mechanism. Biochemistry 2011, 50 (43), 9255–9263. [PubMed: 21939270]
7. Peters JW; Stowell MHB; Soltis SM; Finnegan MG; Johnson MK; Rees DC, Redox-Dependent Structural Changes in the Nitrogenase P-Cluster. Biochemistry 1997, 36 (6), 1181–1187. [PubMed: 9063865]
8. Corbett MC; Hu Y; Fay AW; Tsuruta H; Ribbe MW; Hodgson KO; Hedman B, Conformational Differences between *Azotobacter vinelandii* Nitrogenase MoFe Proteins as Studied by Small-Angle X-Ray Scattering. Biochemistry 2007, 46, 8066–8074. [PubMed: 17567155]
9. Hu Y; Ribbe MW, Biosynthesis of the Metalloclusters of Nitrogenases. Annu. Rev. Biochem 2016, 85, 455–483. [PubMed: 26844394]
10. Hu Y; Corbett MC; Fay AW; Webber JA; Hedman B; Hodgson KO; Ribbe MW, Nitrogenase Reactivity with P-Cluster Variants. Proc. Natl. Acad. Sci. U. S. A 2005, 102 (39), 13825–13830. [PubMed: 16166259]
11. Hu Y; Fay AW; Lee CC; Ribbe MW, P-Cluster Maturation in Nitrogenase MoFe Protein. Proc. Natl. Acad. Sci. U. S. A 2007, 104 (25), 10424–10429. [PubMed: 17563349]
12. Broach RB; Rupnik K; Hu Y; Fay AW; Cotton M; Ribbe MW; Hales BJ, VTVH-MCD spectroscopic Study of the Metal Clusters in the Δ*nifB* and Δ*nifH* MoFe Proteins of Nitrogenase from *Azotobacter vinelandii*. Biochemistry 2006, 45, 15039–15048. [PubMed: 17154541]
13. Rupnik K; Lee CC; Hu Y; Ribbe MW; Hales BJ, $[4Fe4S]^{2+}$ Clusters Exhibit Ground-State Paramagnetism. J. Am. Chem. Soc 2011, 133, 6871–6873. [PubMed: 21488637]
14. Rupnik K; Lee CC; Wiig JA; Hu Y; Ribbe MW; Hales BJ, Nonenzymatic Synthesis of the P−Cluster in the Nitrogenase MoFe Protein: Evidence of the Involvement of All-Ferrous $[Fe_4S_4]^0$ Intermediates. Biochemsitry 2014, 53, 1108–1116.
15. Corbett MC; Hu Y; Naderi F; Ribbe MW; Hedman B; Hodgson KO, Comparison of iron-molybdenum cofactor deficient nitrogenase MoFe proteins by X-ray absorption spectroscopy:

Implications for P-cluster biosynthesis. J. Biol. Chem 2004, 279, 28276–28282. [PubMed: 15102840]

16. Lee CC; Blank MA; Fay AW; Yoshizawa JM; Hu Y; Hodgson KO; Hedman B; Ribbe MW, Stepwiese formation of P-clusters in nitrogenase MoFe protein. Proc. Natl. Acad. Sci. U. S. A 2009, 106, 18474–19478. [PubMed: 19828444]
17. Cotton MS; Rupnik K; Broach RB; Hu Y; Fay AW; Ribbe MW; Hales BJ, VTVH-MCD Study of the ΔnifBΔnifZ MoFe Protein from Azotobacter vinelandii. J. Am. Chem. Soc 2009, 131, 4558–4559. [PubMed: 19334767]
18. Hu Y; Fay AW; Dos Santos PC; Nader F; Ribbe MW, Characterization of *Azotobacter vinelnadii nifZ* Deletion Strains. J. Biol. Chem 2004, 279 (52), 54963–54971. [PubMed: 15485884]
19. Johnson MK, CD and MCD Spectroscopy In Physical Methods in Bioinorganic Chemistry; Spectroscopy and Magnetism, Lawrence Que J, Ed. University Science Books: Sausalito, CA, 2000; pp 233–286.
20. Johnson MK; Robinson AE; Thomson AJ, Low-Temperature Magnetic Circular Dichroism Studies of Iron-Sulfur Proteins In Iron-Sulfur Proteins, Spiro TG, Ed. Wiley-Interscience: New York, NY, 1982; pp 367–406.
21. Onate YA; Finnegan MG; Hales BJ; Johnson MK, Variable Temperature Magnetic Circular Dichroism Studies of Reduced Nitrogenase Iron Proteins and $[4Fe\text{-}4S]^{+}$ Synthetic Analog Clusters. Biochim. Biophys. Acta 1993, 1164, 113–123. [PubMed: 8329442]
22. Rupnik K; Hu Y; Lee CC; Wiig JA; Ribbe MW; Hales BJ, P^{+} State of Nitrogenase P-Cluster Exhibits Electronic Structure of a $[Fe_4S_4]^{+}$ Cluster. J. Am. Chem. Soc. 2012, 134, 13749–13754. [PubMed: 22839751]
23. Rebelein JG; Stiebritz MT; Lee CC; Hu Y, Activation and reduction of carbon dioxide by nitrogenase iron proteins. Nat. Chem. Biol. 2017, 13 (2), 147–149. [PubMed: 27893704]
24. Ribbe MW; Burgess B, The chaperone GroEL is required for the final assembly of the molybdenum-iron protein of nitrogenase. Proceedings of the Academy of Natural Sciences, U. S. A 2001, 98 (10), 5521–5525.

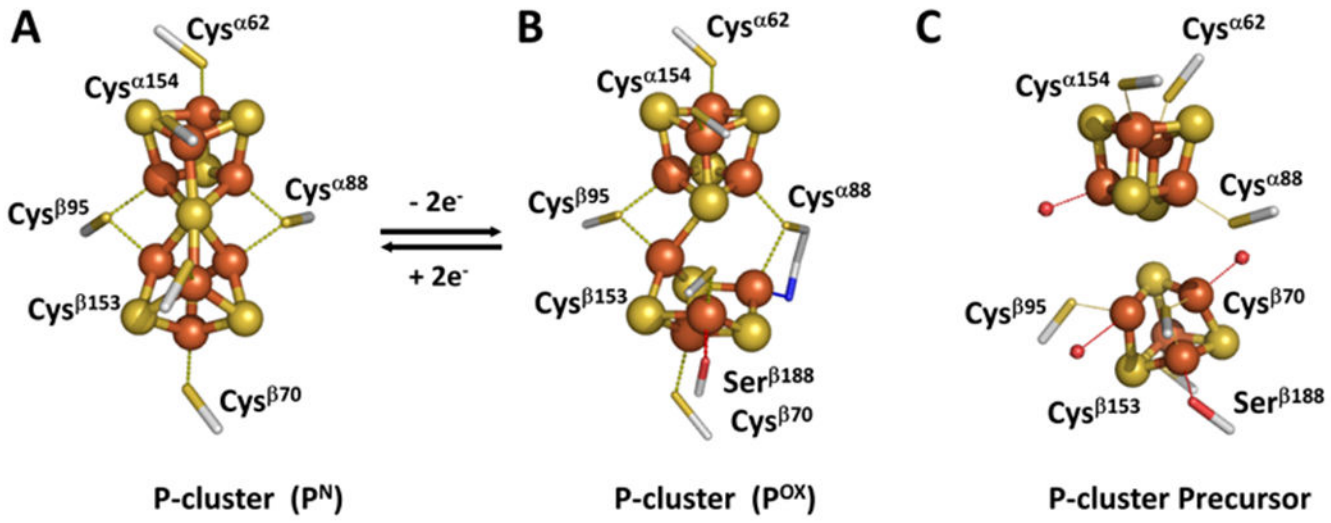

Figure 1.

Structures of the P-cluster in the reduced, P^N (A) and oxidized, P^{2+} (B) states and the P-cluster precursor in ΔnifH and ΔnifBZ MoFe proteins (C). The structures shown in A and B are crystallographic observations[7] and the structure shown in C is an XAS/EXAFS-derived model[8].

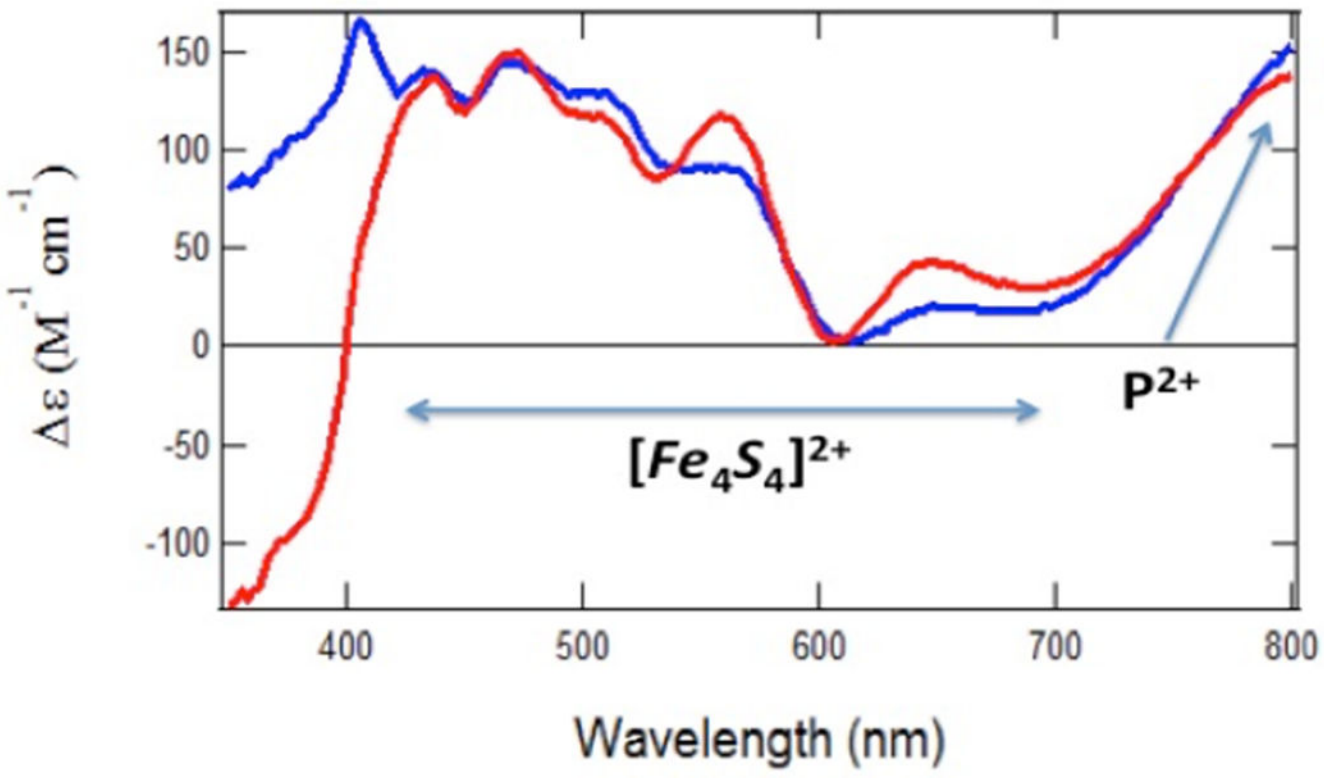

Figure 2.

Comparison between the MCD spectrum of IDS-oxidized Δ*nifBZ* MoFe protein (red) and a simulated MCD spectrum (blue; 80 mg/mL) generated by adding ½ of the spectrum of IDS-oxidized Δ*nifB* MoFe protein (representing one P^{2+} signal; 14.5 mg/mL) and ½ of the spectrum of IDS-oxidized Δ*nifH* MoFe protein (representing two paramagnetic $[Fe_4S_4]^{2+}$ clusters; 34 mg/mL). The strong similarity between the two spectra shows that the $[Fe_4S_4]^{2+}$ clusters in Δ*nifBZ* MoFe protein remain paramagnetic as they are in Δ*nifH* MoFe protein. Spectra were recorded at 1.6 K and 6.0 T.

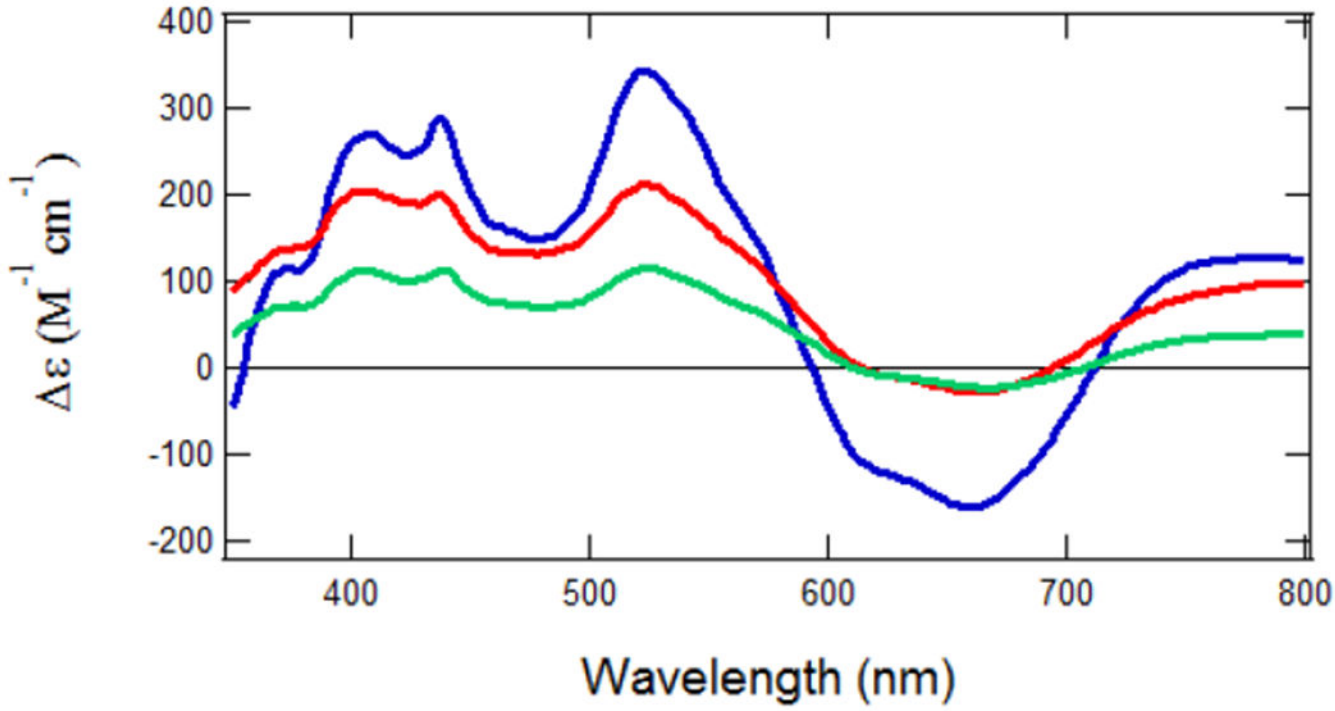

Figure 3.

MCD spectra of dithionite-reduced Δ*nifH* MoFe protein (blue; 70 mg/mL), Δ*nifBZ* MoFe protein (red; 40 mg/mL) and Δ*nifBZ* MoFe protein^{+NifZ} (green; 76 mg/mL). Spectra were recorded at 1.6 K and 6.0 T.

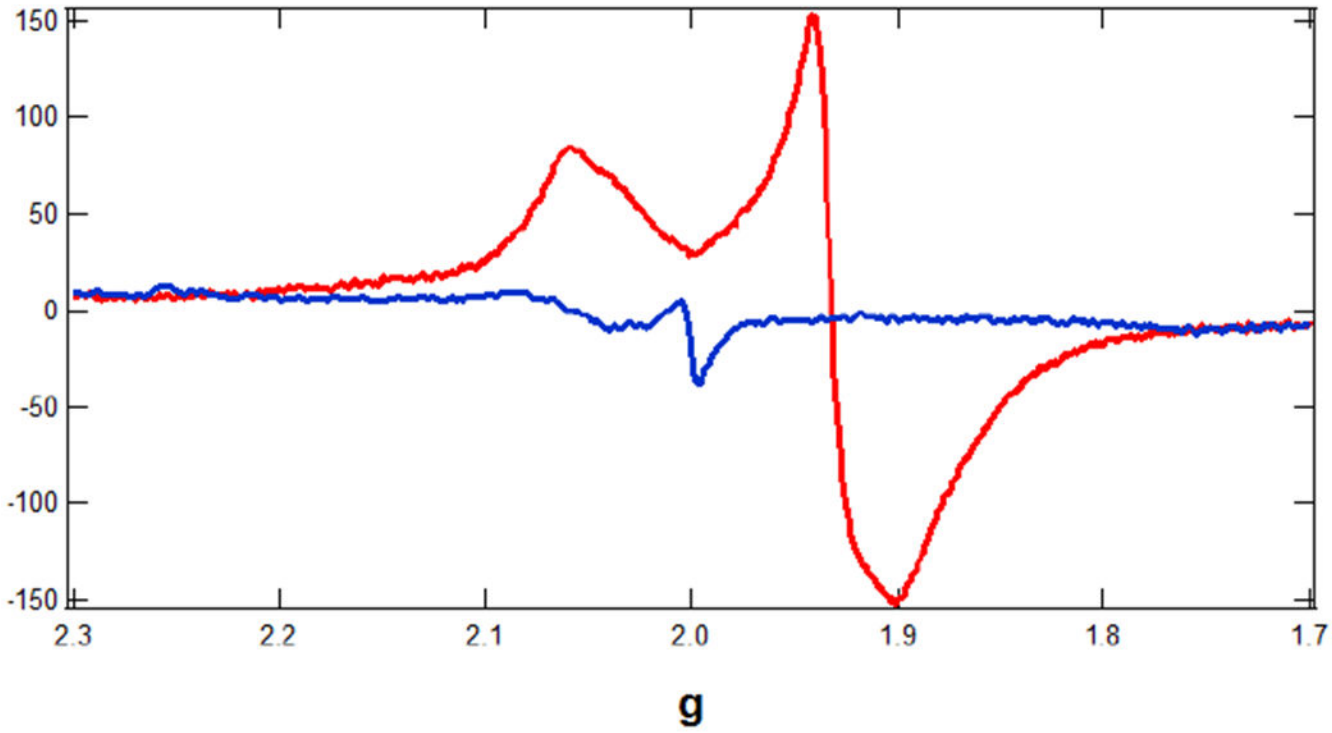

Figure 4.

EPR spectra of dithionite-reduced Δ*nifBZ* MoFe protein (red) and Δ*nifBZ* MoFe protein $^{+NifZ}$ (blue). Spectra were recorded at 9.48 GHz, 10 K, 25 mW microwave power and modulation amplitude of 0.5 mT.

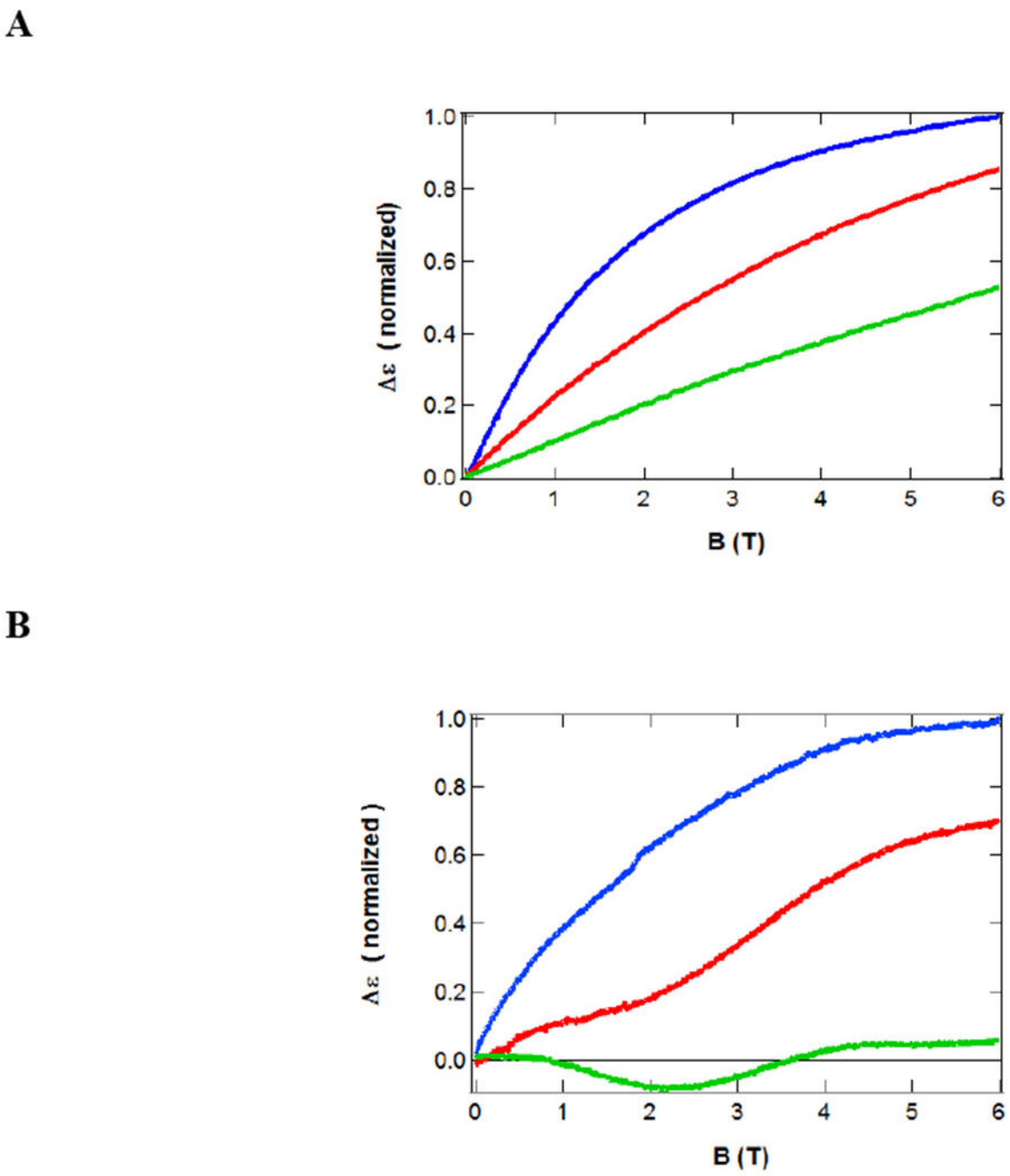

Figure 5.

MCD magnetization curves (plotted versus ***B*** rather than the usual $\beta B/kT$) of dithionite-reduced Δ*nifBZ* MoFe protein before (A) and after (B) incubation with NifZ. The magnetization curves of Δ*nifBZ* MoFe protein (A) represent the sum of the paramagnetic contribution (**C** term) of the $[Fe_4S_4]^+$ clusters and the linear diamagnetic contribution (**B** term) of the P^N cluster. Upon incubation with NifZ, the magnetization curves of Δ*nifBZ* MoFe protein^{+NifZ} (B) show a distinct curvature at higher temperatures. The magnetization

curves were recorded at 520 nm, 6 T and 1.6 K (blue), 4.2 K (red) and 10 K (green), respectively.

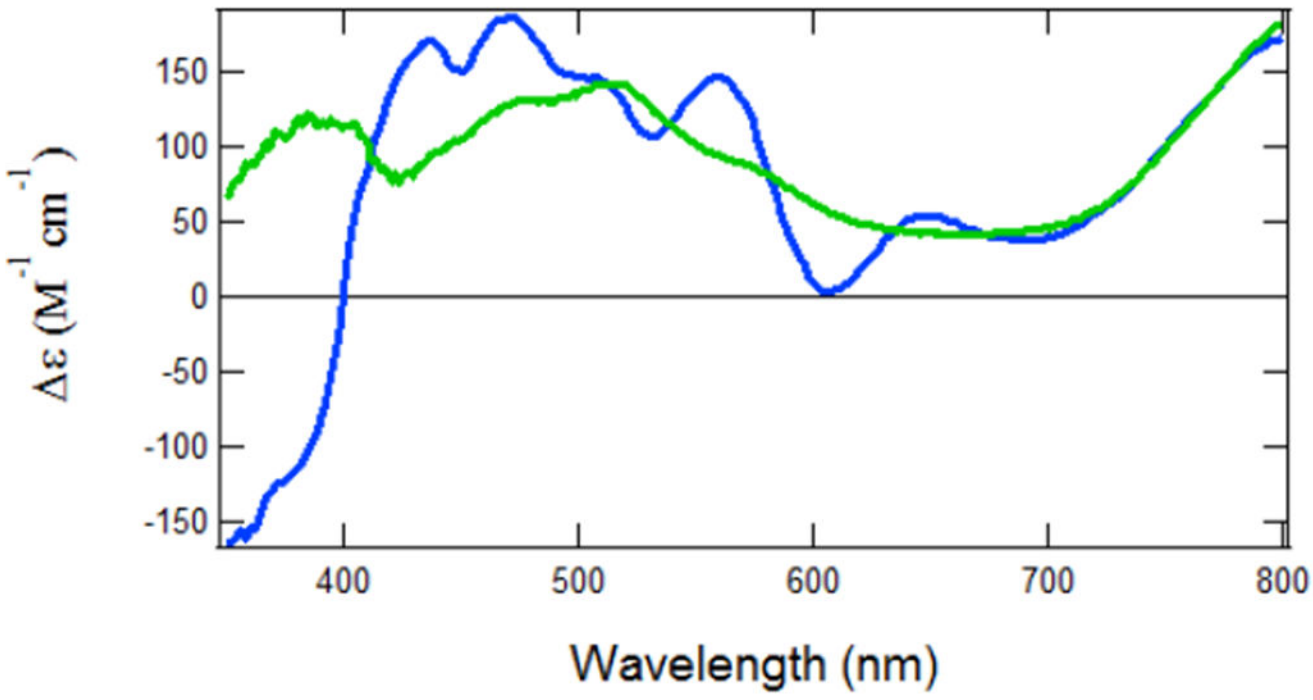

Figure 6.

Comparison between the MCD spectrum of IDS oxidized IDS-oxidized Δ*nifBZ* MoFe protein^{+NifZ} (green; 71 mg/mL) and the simulated spectrum (blue) generated by adding ½ of the spectrum of IDS-oxidized Δ*nifB* MoFe protein (representing one P^{2+} signal; 14.5 mg/mL) and ¼ of the spectrum of IDS-oxidized Δ*nifH* MoFe protein (representing one paramagnetic $[Fe_4S_4]^{2+}$ cluster; 34 mg/mL). The lack of structure associated with the paramagnetic $[Fe_4S_4]^{2+}$ cluster (see Figure 2) in the spectrum of Δ*nifBZ* MoFe protein^{+NifZ} shows that, like all other classic $[Fe_4S_4]^{2+}$ clusters, the $[Fe_4S_4]^{2+}$ cluster in Δ*nifBZ* MoFe protein^{+NifZ} is now diamagnetic. Spectra were recorded at 1.6 K and 6.0 T.

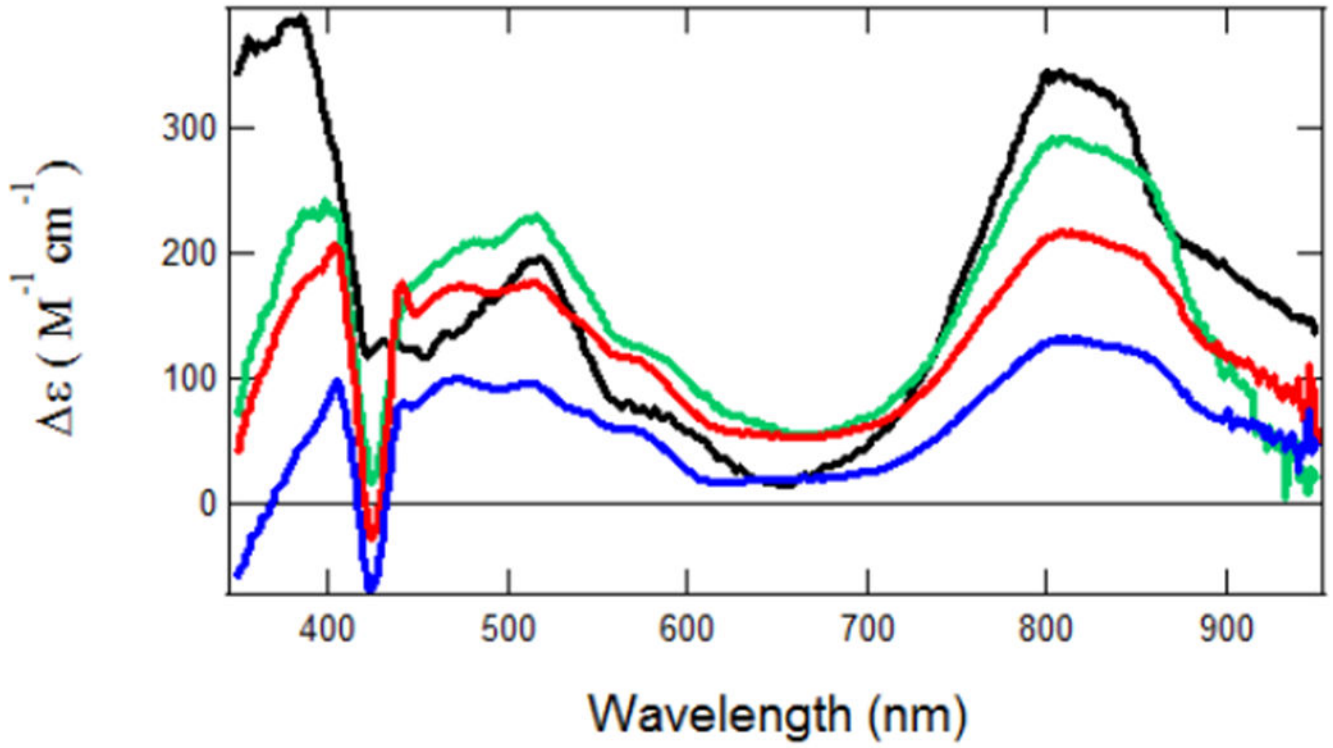

Figure 7.

MCD spectra recorded during the biosynthesis of the two P-clusters in the IDS-oxidized Δ*nifH* MoFe protein at 5 min (blue; 40.1 mg/mL), 20 min (red; 58mmg/mL) and 60 min (green; 79.3 mg/mL) in comparison with the MCD spectrum of Δ*nifB* MoFe protein (black; 56 mg/mL) that contains two P-clusters. Note that the intensity of the P^{2+} clusters seen at 800 nm increases with time as the P-clusters are being synthesized. During the synthesis of the P-cluster, inflections arise in the 400–600 nm region, which are not associated with the P^{2+} cluster, but possibly associated with the predicted intermediate(s) ***A*** and/or ***B***. Spectra were recorded at 1.6 K and 6.0 T.

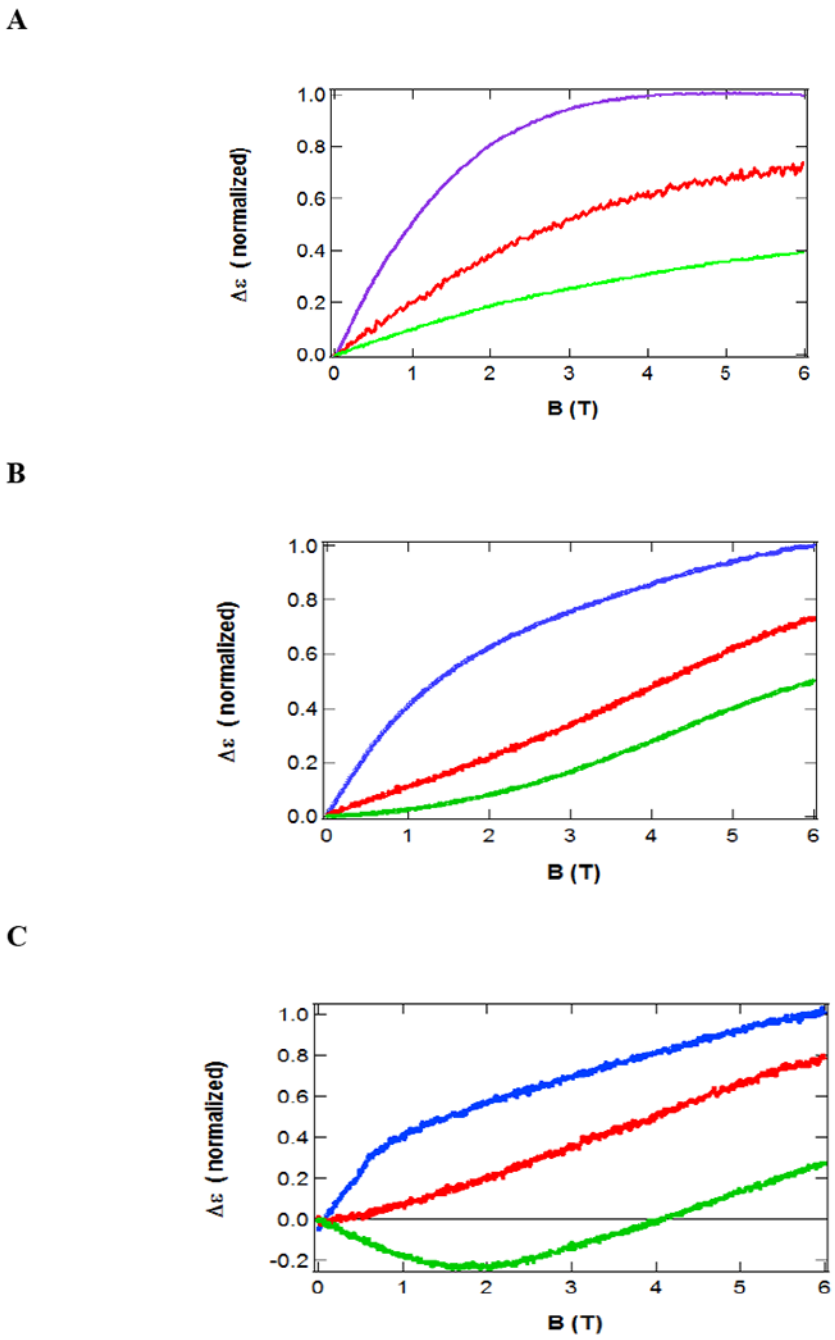

Figure 8.

MCD magnetization curves (plotted versus ***B*** rather than the usual $\beta B/kT$) recorded during the biosynthesis of the two P-clusters in the dithionite-reduced Δ*nifH* MoFe protein at 0 min (A), 5 min (B) and 20 min (C). Spectra were recorded at 520 nm, 6.0 T and 1.6 K (blue), 4.2 K (red) and 10 K (green), respectively. Note that the curves at 1.6 K closely mimic the curves of a standard $S = ½$ spin system, whereas the curves at 4.2 K and 10 K show strong deviations from an $S = ½$ system, suggesting the presence of another spin system that is likely integer.

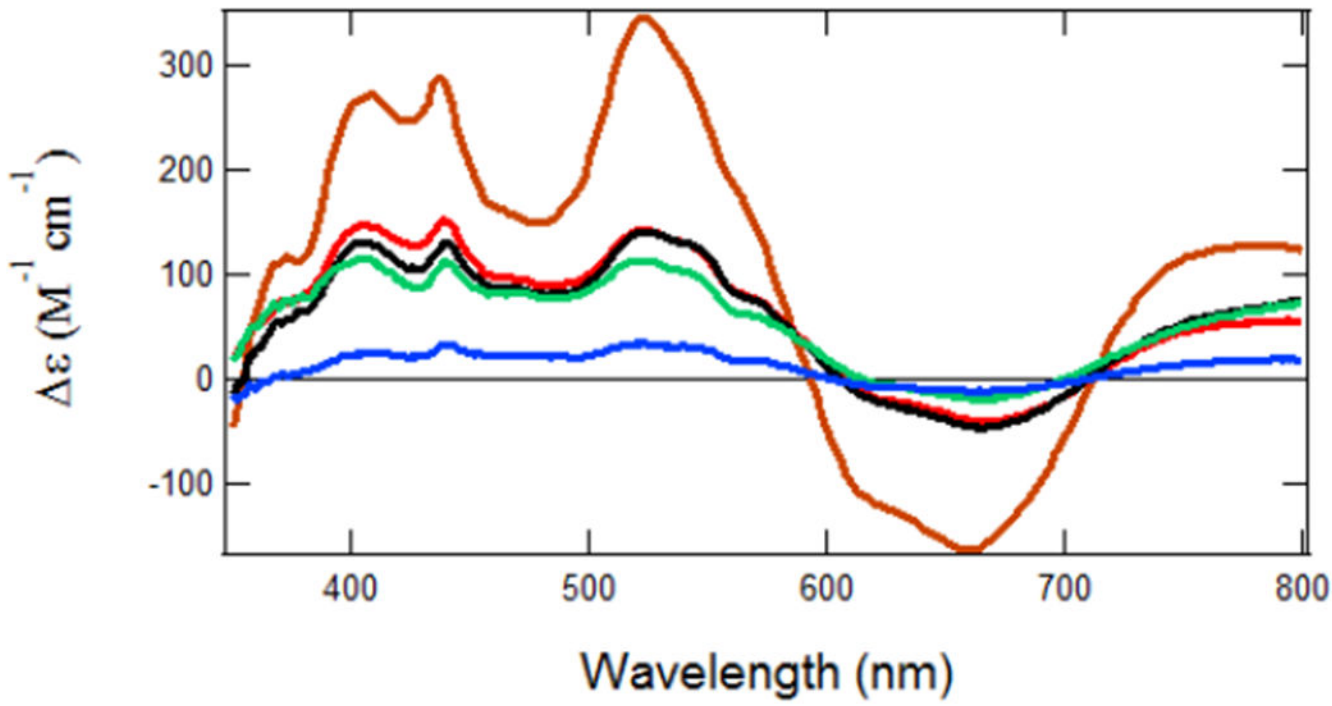

Figure 9.

MCD spectra recorded during the biosynthesis of the two P-clusters in the dithionite-reduced Δ*nifH* MoFe protein at 0 min (black; 113.2 mg/mL), 5 min (red), 20 min (blue), 60 min (green) and 120 min (brown). Note that the intensity of the $[Fe_4S_4]^+$-like spectrum decreases in the first 20 min but increases afterwards to *ca.* 2 clusters per protein. Spectra were recorded at 1.6 K and 6.0 T.

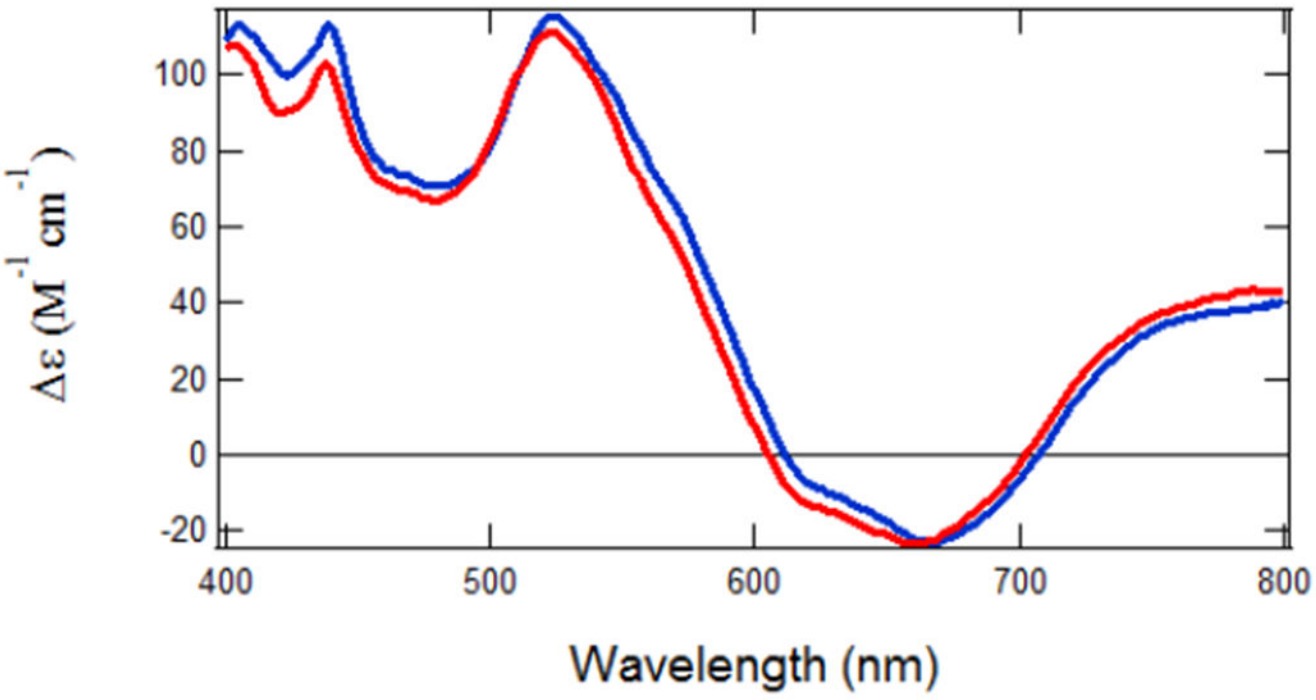

Figure 10.

Comparison between the MCD spectrum of dithionite-reduced Δ*nifBZ* MoFe protein^{+NifZ} (blue) and a simulated spectrum (red) generated by adding ½ the spectrum of the dithionite-reduced Δ*nifBZ* MoFe protein (representing one $[Fe_4S_4]^+$ cluster) and ¼ the spectrum of the Ti(III) citrate-reduced Δ*nifH* MoFe protein (representing one $S = 4$ $[Fe_4S_4]^0$ cluster).

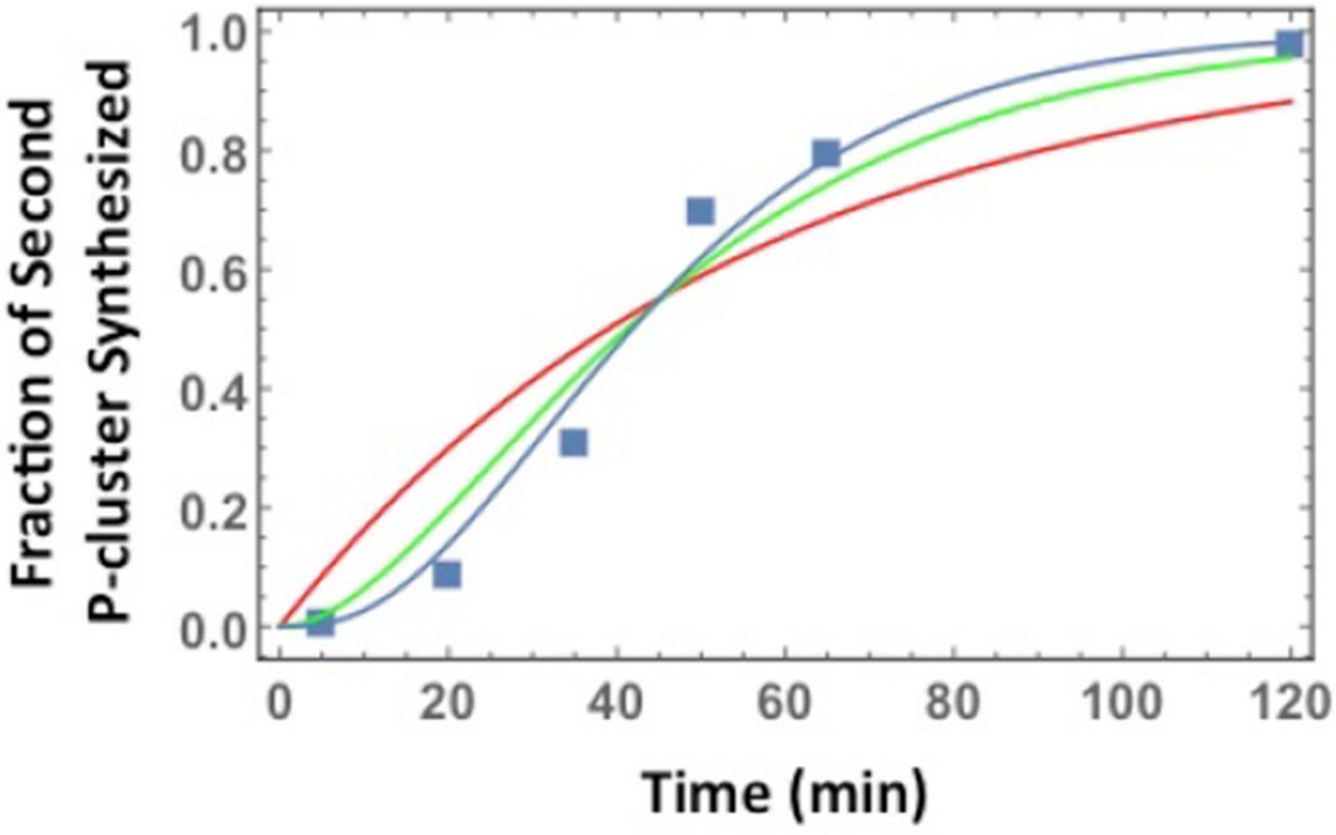

Figure 11.

Best-fit theoretical predictions of the time-dependent concentration increase of the second P-cluster, assuming no intermediate (Eq. SE1; red), one intermediate (Eq. SE14; green) or two intermediates (Eq. SE15; blue). The average data (blue squares) from EPR spectroscopic studies and activity measurements are also shown in the figure.

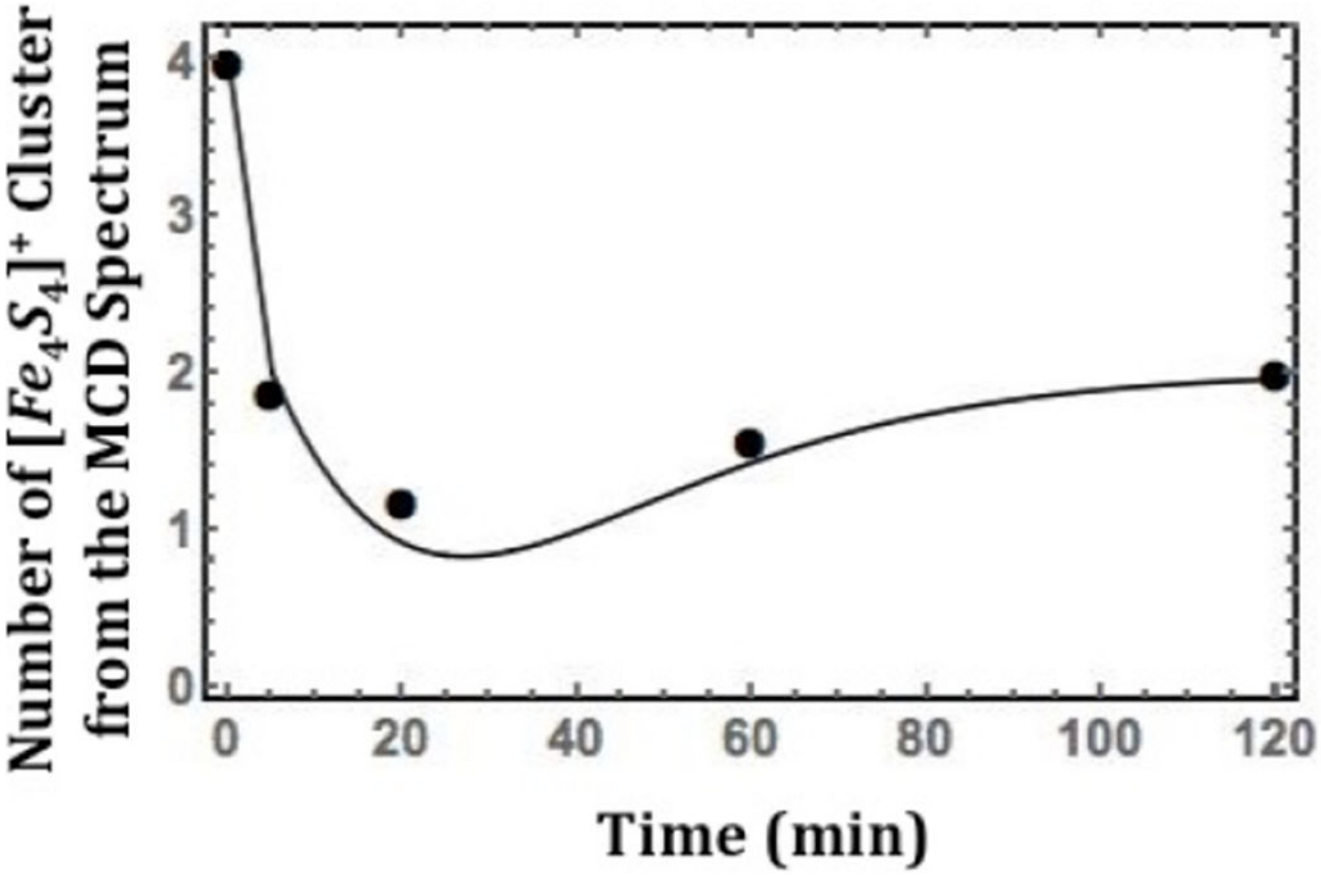

Figure 12.

Theoretical plot (solid line) of the MCD signal of the reduced Δ*nifH* MoFe protein *versus* time (using Eqs. SE7, SE11, SE12 and SE13) assuming the new $[Fe_4S_4]^+$-like spectrum is formed in parallel with the synthesis of the second P-cluster. Amplitudes (at 520 nm) of experimental MCD spectra are shown as black circles.